Revista Brasileira de Geofísica
RBGf
Brazilian Journal of Geophysics

MAPPING IRON-MINERALIZED LATERITE ENVIRONMENTS BASED ON TEXTURAL ATTRIBUTES FROM MAPSAR IMAGE SIMULATION – SAR-R99B (SIVAM/SIPAM) IN THE AMAZON REGION

Maria Carolina de Morais[1], Paulo Pereira Martins Junior[1,2] and Waldir Renato Paradella[3]

ABSTRACT. The use of remote sensing is a valuable method for geological mapping as it provides synoptic coverage at relatively low cost. In the Amazon region, radar imagery has a potential for geological applications due the enhanced sensitivity to topography (macrotopography), surface roughness (microtopography), and dielectric properties of materials, independent of weather, sun angle, and illumination conditions. As the roughness is highlighted, SAR textural attributes can be used for mapping iron-ore mineralized laterites in N1 deposit, located in the Carajás Province. For mapping the lateritic cover, the airborne SAR was used from Surveillance of the Amazon System (SIVAM/SIPAM, L-hh, L-hv, L-vv) to simulate orbital Multi-Application Purpose SAR (MAPSAR). The images were analyzed through textural classifications derived from second-order measure (GLCM) with the objective of mapping the mineralized laterites for iron ore. Differences are highlighted when comparing the classified maps and the ground information. Not all classes were separated, but a high performance for textural attributes was presented by the hematite class. This class was sensitive to the sensor and target parameters, especially macrotopography and physics characteristics. The results showed that for mineral exploration, the radar images at L-band can be used as a practical tool for a preliminary mapping, and as a guide for field-based verification.

Keywords: Amazônia, SAR, MAPSAR, textural attribute, laterite cover, SIVAM/SIPAM, L-hh, L-hv, L-vv.

RESUMO. Imagens de radar são úteis em geologia devido à visão sinóptica e a uma cobertura a um custo relativamente baixo. Particularmente na região amazônica, o uso de imagens de radar em aplicações geológicas é favorecido pela capacidade de realce do relevo (macrotopografia), da rugosidade superficial (microtopografia) e da constante dielétrica, independente da presença de nuvens, ângulo solar e condições de iluminação. A microtopografia do terreno, realçada neste tipo de imagem, permite que a textura das imagens de radar possa ser usada no mapeamento das coberturas lateríticas mineralizadas em ferro do depósito N1, localizado na Província de Carajás. A investigação se baseou em imagens adquiridas por radar aerotransportado (SIVAM/SIPAM, banda L-hh, L-hv e L-vv), cujas faixas de voo foram degradadas visando à simulação do SAR orbital MAPSAR. Os dados foram analisados através de classificações texturais, derivadas de medidas obtidas por meio de Matriz de Co-ocorrência dos Níveis de Cinza (MCNC) com o objetivo de mapeamento das unidades lateríticas em N1. Muitas diferenças foram encontradas entre as classes mapeadas e o mapa de verdade terrestre. Nem todas as classes foram separadas, mas a hematita apresentou alto desempenho na classificação. Esta classe foi sensível aos parâmetros do alvo e do sensor, especialmente a macrotopografia e as características físicas. Os resultados mostraram que a classificação baseada em MCNC pode ser usada como ferramenta preliminar de mapeamento das lateritas e como um guia para verificação de campo.

Palavras-chave: Amazônia, Radar de Abertura Sintética, MAPSAR, atributo textural, cobertura laterítica, SIVAM/SIPAM, L-hh, L-hv, L-vv.

[1]Federal University of Ouro Preto (UFOP), School of Mines, Department of Geology (DEGEO), Campus Universitário Morro do Cruzeiro, s/n, Bauxita, 35400-000 Ouro Preto, MG, Brazil. Phone/Fax: +55 (31) 3559-1601 – E-mail: mdemorais@gmail.com

[2]Minas Gerais Technological Center Foundation (CETEC), Water Resources Sector (SAA), Av. José Cândido da Silveira, 2000, Horto, 31170-000 Belo Horizonte, MG, Brazil. Phone/Fax: +55 (31) 3489-2250; Fax: +55 (31) 3489-2227 – E-mail: maerteyn@gmail.com

[3]National Institute for Space Research (INPE), Remote Sensing Division (DSR), Av. dos Astronautas, 1758, 12227-010 São José dos Campos, SP, Brazil. Phone/Fax: +55 (12) 3945-6438 / +55 (12) 3945-6400 – E-mail: waldir@ltid.inpe.br

INTRODUCTION

The Carajás Mineral Province is located on the easternmost border of the Amazon region. It is one of most important mineral provinces in the world, with a predominating iron production and enormous potentials for Mn, Cu, Au, Ni, U, Ag, Pd, Pt, Os, and others (Lobato et al., 2005). This mineral province area is on a mountainous terrain with altitudes higher than 900 m, surrounded by southern and northern lowlands with altitudes around 150-200 m with thick oxisols ("latosols") as a result of deep chemical weathering and with few rocks outcrops. The vegetation cover is typical of the Equatorial forest with complex, multilevel canopies and numerous species (Paradella et al., 1994).

Since 1967, when the iron deposits were discovered, a remarkable geobotanical contrast given by the iron-mineralized laterites and specific vegetation types has been recognized. The deposits are related to a set of plateaux covered by thick hard iron-rich crusts developed over volcanic rocks and ironstones. A specific low-density *campos rupestres* vegetation (Silva et al., 1986) is associated with the deposits, and shows a strong contrast with the dense equatorial forest. This contrast was detectable through radar airborne C-band imageries during the SAREX'92 (South American Radar Experiment'92) campaigns (Morais et al., 2002). The province was almost completely covered during the SAREX'92 campaign in preparation for ERS-2 and RADARSAT-1 launches. Details of the SAREX'92 can be found in Wooding et al. (1993).

In the Amazon region, C-band backscatter intensity is strongly controlled by decameter scale changes in the surface slope, and by centimeter scale roughness characteristics of the crown scattering, including multiple scattering within the crowns. The preliminary evaluation, by textural classifications, of this SAR data has shown that the backscattered C-band responses are sensitive to this geobotanical contrast in depicting variations in the duricrust vegetation associations (Morais et al., 2002).

Due to the economic importance of this area, there is a practical need to provide accurate and up-to-date surface maps to support mineral exploration and environmental programs. The province has been extensively covered by various airborne (RADAMBRASIL, INTERA, SAREX) and spaceborne SAR (ERS-1, JERS-1, RADARSAT-1) surveys. These data have played an important role in the acquisition of geological information in the Carajás Province (Paradella et al., 1997, 2000). In addition, with SAR system satellites (ALOS/PALSAR and RADARSAT-2) having new characteristics (resolution, polarization, incidence, wavelength) the practical utility of textural SAR classification for mapping remains to be demonstrated.

The Brazilian-German MAPSAR (Multi-Application Purpose SAR) is a proposal for an innovative L-band sensor whose main mission is to assess and monitor natural resources. The MAPSAR mission is a small spaceborne SAR conceived by Brazilian-German scientific and technical cooperation between INPE (*Instituto Nacional de Pesquisas Espaciais*) and DLR (*Deutschen Zentrums für Luft- und Raumfahrt*) (Schröder et al., 2005). Even before its lauching, imagery simulation was an important aspect for the potential-use investigation of SAR. Thus, before its launching, the simulation of MAPSAR imagery is now performed by using images provided by the airborne SAR L-Band sensor, the R99 of the SIVAM/SIPAM (Surveillance of the Amazon System) (Schröder et al., 2005). In this stage, a set of test sites was selected covering fields like Agriculture, Forestry, Geology and Mineral Exploration, Disaster Management, Coastal Zone Studies, Geomorphology, Hydrology and Environmental Analysis.

The images of the Carajás Mineral Province were acquired on June 2005 as part of this campaign. The area was covered in June 2005 by an airborne SAR-R99B with adapted processing and simulation techniques to simulate the expected MAPSAR imagery products. Since the lateritic compositions play an important role in the expression of the macro and micro topographical roughness, it was considered worthwhile to evaluate the SAR texture obtained from MAPSAR L-band on lateritic crust.

The main objective was mapping iron ore laterites from the N1 Deposit in Carajás Mineral Province through MAPSAR imagery simulation. The research used the L-band with the expectation that this proposed approach could be used as a tool for mapping other similar areas.

STUDY AREA

The N1 is an iron-ore deposit located in the Carajás Mineral Province, on the easternmost border of the Amazon region (Fig. 1). The total ore resources for the Carajás Province are estimated to be 17.8 billion tons having a 66.1% iron concentration (Beisiegel et al., 1973). The N1 deposit is a plateau with altitudes of around 700 m and an approximate area of 24 km^2.

The N1 deposit is related to rocks of the Grão Pará Group, displaying complex patterns of folding and faulting. The Grão Pará Group has been subdivided into two units: volcanic rocks of the Parauapebas Formation (Meirelles et al., 1984), and the ironstones of the Carajás Formation (Beisiegel et al., 1973). The volcanic rocks are a bimodal sequence of basalts, dolerites and rhyolites. The ironstones of the Carajás Formation are composed of several types of iron ore of various oxide facies. They are mainly jaspilite and interlayered hematite and silica (Tolbert
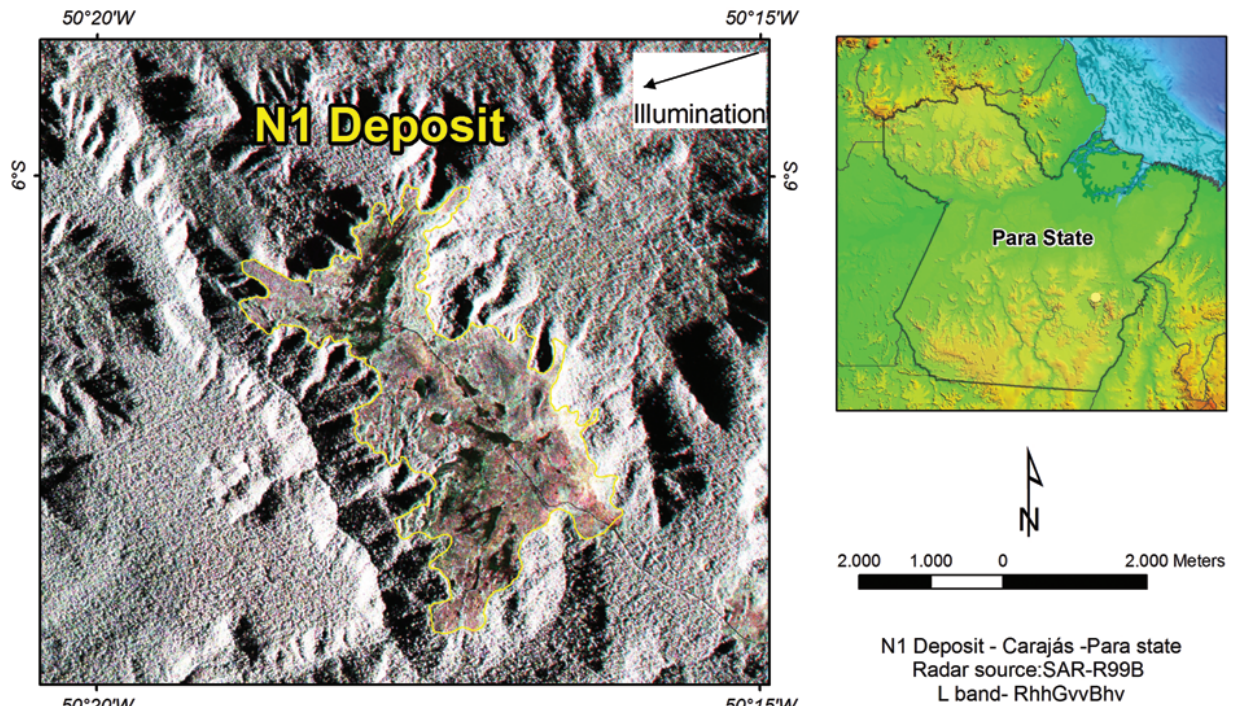
Figure 1 – Location map of N1 deposit.

et al., 1971), which are either of soft or hard hematite (Lobato et al., 2005). The jaspilites have variable compositions with 17.11-43.40% Fe and 35.10-60.84% SiO_2 presenting typical interlayering of dark and light centimetre-thick mesobands and microbanding with iron-oxide layers intercalated with white to pale or bright red layers composed of crypto to microcrystalline SiO_2 (jasper and chert) with inclusions of cryptocrystalline hematite (Tolbert et al., 1971; Beisiegel et al., 1973).

Under the humid tropical climate of the Amazon region, ferruginous and latosoils are extensively developed in the plateau. These weathered products show varying degrees of alteration that are responsible for the differences in composition, hardness and textures. The N1 area was mapped during the economic evaluation of the iron reserves in the province (Resende & Barbosa, 1972). The following types of ferruginous crusts were identified in the area: duricrust (*in situ* duricrust with limonite blocks), chemical crust (hematite fragments with goethitic pisolites), iron-ore duricrust (hematite ore blocks and subordinately specularite, cemented with hydrous ferric oxides), and hematite (mainly hematite outcrops). In addition, a latosoil unit was also mapped in a restricted area, associated with arboreal vegetation. The surface map of the plateau is seen in Figure 2.

Situated on rock outcrops N1 vegetation has a typical aspect of the tropical scrubs called *campos rupestres* (Silva et al., 1986).

It is predominantly composed of herbs and arboreal plants types with less development of the semi-arboreal type. Semi-arboreal ecosystems are common in restrict lands; others areas have arboreal species strictly found in latosoil. *Gramineae* and *Leguminosae* plant families have a large geographic distribution. A geobotanical control is evident in N1 ferruginous area showing relations between vegetation and relief that support the crusts (Silva et al., 1986). As seen in Figure 3, on the top of the hills with many rock outcrops a layer of soil is very restricted and plant species are of short types. Coming down the hills it is common to see some soil and organic matter, which permit the development of plant species of higher sizes in fissures over the crusts. On the basis of the hills the flora attains its maximum development with a major growth of species. Many lakes are covered by a vegetation of the *Typha* sp. type regionally known as "taboa", where outcrops of the crusts are exposed during the dry seasons.

DATASET

The research was based on airborne SAR imagery obtained from the Amazon Surveillance System (SIVAM/SIPAM, L-hh, L-hv, L-vv) aiming for the simulation of orbital Multi-Application Purpose SAR (MAPSAR) used for the assessment and monitoring of natural resource applications in the Amazon region. The characteristics of SAR-R99B data are shown in Table 1.
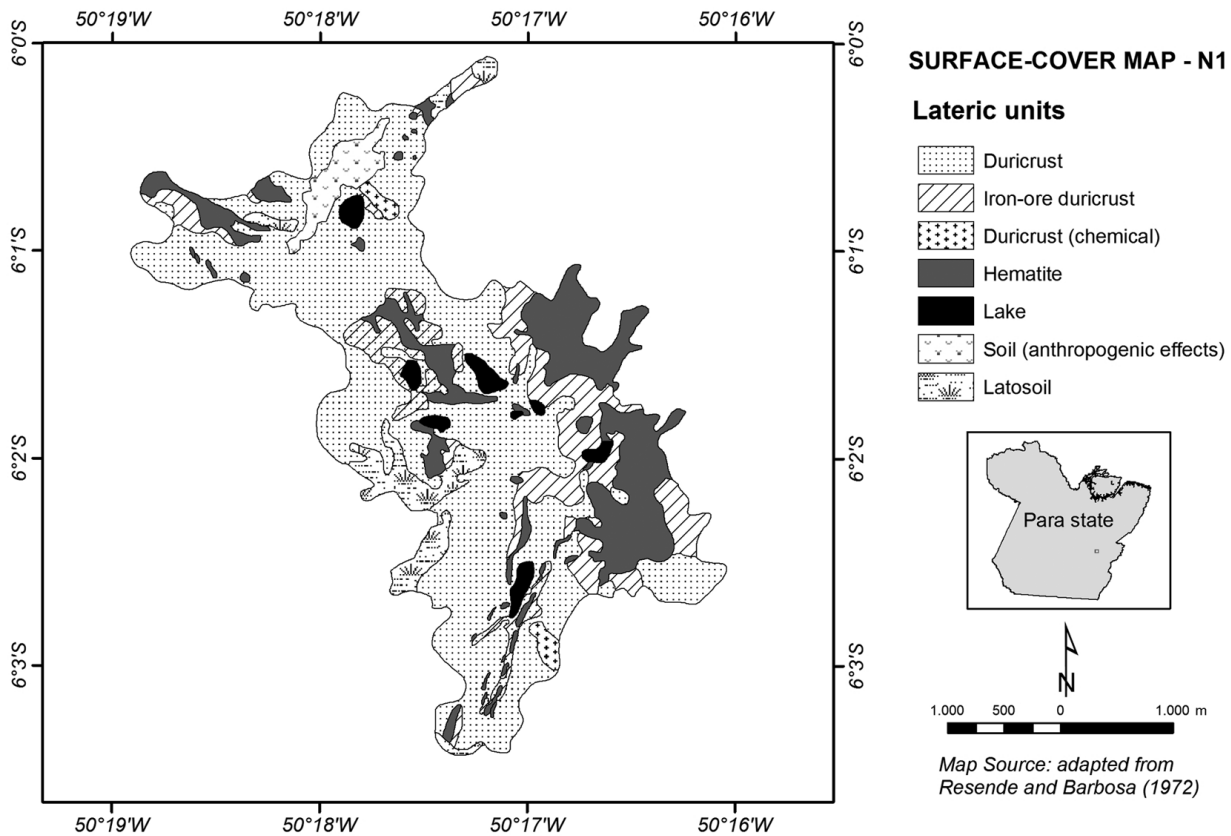
SURFACE-COVER MAP - N1

Lateric units

- Duricrust
- Iron-ore duricrust
- Duricrust (chemical)
- Hematite
- Lake
- Soil (anthropogenic effects)
- Latosoil

Para state

1.000 500   0   1.000 m

Map Source: adapted from Resende and Barbosa (1972)

Figure 2 – Surface-Cover Map from N1 plateau adapted from Resende & Barbosa (1972).

Table 1 – SAR-R99B characteristics.

Parameter	Specification
Platform	EMB-145
Band	L
Polarization	hh, hv, vv
Acquisition Date	June 2005
Incident Angle (deg)	48/53°
Spatial Resolution (m)	11 × 11
Image Format	8-bits
Illumination Geometry	Look Azimuth: 282°

METHODOLOGY

The research was based statistical approach known as Grey Level Co-occurrence Matrix (GLCM) proposed by Haralick (1979). Grey tone spatial dependence approach characterises texture by the spatial relationships among grey tones in a local area. Grey tone co-occurrence can be specified in a matrix of relative frequencies P_{ij} in which two neighbouring resolution cells separated by distance d occur on the image, one with grey tone i and the other with grey tone j. Such matrices of spatial grey tone dependence frequencies are symmetric and are a function of the angular relationship between the neighbouring resolution cells as well as a function of the distance between them (Haralick, 1979). Several statistical parameters can be extracted from the GLCM, which can be used as input data in an automatic classification process. Weska et al. (1976), and Welch et al. (1990) consider a class of local properties based on absolute differences between pairs of grey levels. The Grey Level Difference Vector (GLDV) is based on absolute differences between pairs of grey levels i and j at a distance d and at a angle θ.

The textural analysis based on GLCM is a common technique which proved to be effective in earlier studies, e.g. Shanmugan et al. (1981), Ulaby et al. (1986), Yanasse et al. (1993), Baraldi & Parmiggiani (1995), and Kurvonen & Hallikainen (1999), but few examples have focused on the geological applications in tropical environments (Azzibrouck et al., 1997).

The investigation was based on textural descriptors extracted from the GLCM and GLDV used as input for an unsupervised classification scheme. Some of these parameters are related to specific first-order statistical concepts, such as contrast and variance, with clear textural meaning (pixel pair repetition rate, spatial frequencies detection, etc.), while other parameters contain tex-

Schematic croqui showing relations between relief and vegetation on N1 plateau. Source: Silva et al. (1986).
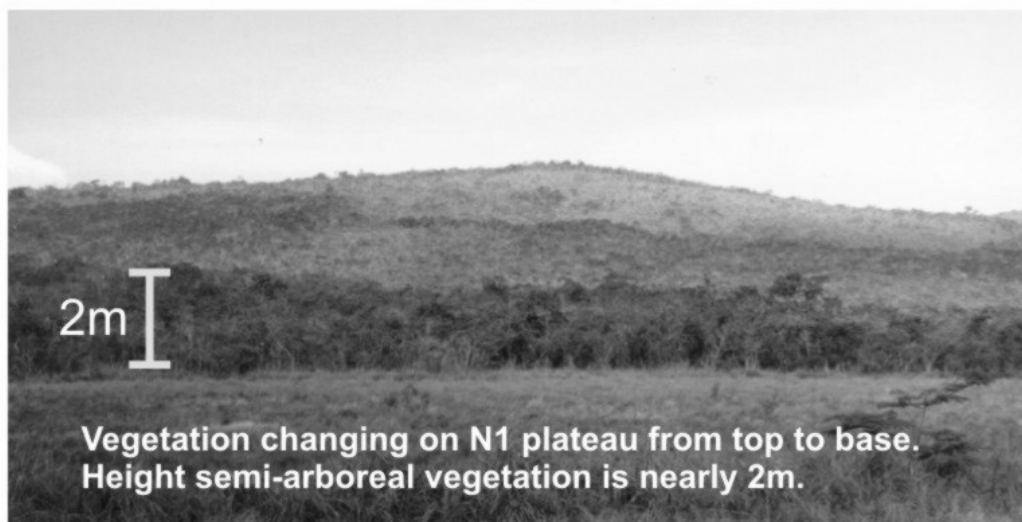
2m

Vegetation changing on N1 plateau from top to base. Height semi-arboreal vegetation is nearly 2m.

Figure 3 – Vegetation changing × relief on N1 plateau.

tural information associated with more than one specific textural meaning (Baraldi & Parmiggiani, 1995).

No speckle filtering was applied to the images in order to keep the original texture of SAR scenes. Representative samples of nine classes were chosen, on the basis of field observations and the mapped surface: C1 = Latosoil, C2 = Soil (anthropogenic effects), C3 = Duricrust (chemical), C4 = Duricrust, C5 = Iron-ore duricrust (with shadow), C6 = Iron-ore duricrust, C7 = Hematite (with shadow), C8 = Hematite, and C9 = Lake. The inclusion of some classes with shadow-effects was necessary since shadow effects were pronounced on the SAR images. Based on these samples, second-order measures derived from GLCM (mean, homogeneity, contrast, dissimilarity, entropy, energy, correlation) and from Grey-Level Difference Vector-GLDV (energy, entropy, mean, contrast) were analyzed. The second-order measures were computed with nine configurations of distance (d), i.e., (–2.0), (–2.1), (–2.2), (–1.2), (0.2),

(1.2), (2.2), (2.1), and (2.0). Since 82 measures were made, it became impracticable to use such a large number of configurations in the classification.

Therefore, texture measure selection was based on the Discriminant Factor decision rule that evaluates the separability between classes which details of method can be found in (Rennó et al., 1998). Thus, for two hypothetical classes A and B, and one texture measure k, the Discriminant Factor was computed according to the variation between and within these classes, given by Equation (1):

$$DF_{AB,k} = \frac{n_A \cdot \sum_{i=1}^{n_A} \left(X_{Ai,k} - \overline{X}_{B,k}\right)^2 + n_B \cdot \sum_{i=1}^{n_B} \left(X_{Bi,k} - \overline{X}_{A,k}\right)^2}{n_A \cdot \sum_{i=1}^{n_A} \left(X_{Ai,k} - \overline{X}_{A,k}\right)^2 + n_B \cdot \sum_{i=1}^{n_B} \left(X_{Bi,k} - \overline{X}_{B,k}\right)^2} \quad (1)$$

where $X_{\omega i,k}$ is the ith sample of class ω for the measure k, $\overline{X}_{\omega,k}$ is the mean value of measure k class ω, and n_ω is the number of samples of class ω.

According Equation (1), the texture measure chosen to separate classes A and B is one that selects the highest value of DF_{AB} for all k, indicating the best separateness for these classes. $DF_{AB,k}$ values near one denote that there is confusion between classes A and B for the texture measure k. Thus, for each pair of nine N1 classes, the best set of measures were selected by the criteria described above, using only high DF, which gave (visually) a good performance for classification.

The next step was to generate selected textural channels using texture analysis. For a better control of the grey levels, the textural channels were processed with 32-bits. A 7×7 window pixel cell size was selected in order to maintain GLCM sensitivity to the smallest details of the targets while reducing both noise effects. An unsupervised ISODATA classifier (Mather, 1987) was used for the classification. The classifications were based on the best sets of texture measures for each polarization isolated (hh, hv, and vv) and combined (hh and hv; hh and vv; hv and vv; hh, hv, and vv). In order to refine the results, a post-classification Mode filter algorithm was also applied.

The classification results were analyzed through a confusion matrix to estimate the amount of correctly and incorrectly classified pixels for each class. The method used to evaluate its accuracy was the kappa coefficient of agreement (Foody, 1992), which was evaluated through test samples extracted from the Surface-Cover Map (see Fig. 2). On each classified map, 48 points were randomly allocated for two classes: hematite and no hematite. The statistic test used to evaluate the significant differences between the two classifications is given by Equation (2). All tests for the significant difference between classification results were carried out at a 95% confidence level. At this level, two results may be considered significantly different if $\Delta \hat{k} > 1.96$ (Benson & DeGloria, 1985).

$$\Delta \hat{k} = \frac{|\hat{k}_1 - \hat{k}_2|}{\sqrt{\hat{\sigma}_\infty^2[\hat{k}_1] + \hat{\sigma}_\infty^2[\hat{k}_2]}} , \qquad (2)$$

where $\hat{k}$ kappa and $\hat{\sigma}_\infty^2[\hat{k}]$ is the variance kappa.

In the radar images, small-scale surface roughness refers to microrelief that may modulate the radar return in flat terrain. The roughness varies with radar wavelengths, incidence angle, and the topography. The roughness may closely relate to underlying geological substrate and may also be caused by weathering processes, by soil composition, or vegetation associations (Werle, 1988).

The roughness is a very important target parameter that influences the performance of the textural classification, and roughness measurements were also collected at 73 representative si-

tes of the main classes. Surface roughness is generally difficult to measure accurately in the field, but the *in situ* measurements were considered a first approximation to categorise lateritic crusts as smooth, intermediate, or rough. The height values from each unit were obtained, in RMS (root mean square) values, by inserting a thin plate into the surface (Fig. 4) photographing it, and digitising the profile. The roughness classification was based on the criterion proposed by (Peake & Oliver, 1971) calculated for local incident angles at L-band wavelength.

RESULTS

For each SAR configuration, Table 2 shows the best selected textural measures used in the classifications with distances d (distance in pixels at considered direction for measures related to GLCM). The mean and GLDV contrast measures were sensitive for all data.

Table 2 – Best selected textural measures with the d distances for each SAR configuration used in the classification.

SAR data	Measures	d
L-hh	Mean	−2.1
	Dissimilarity	1.2
	GLDV contrast	1.2
	GLDV energy	2.1
L-hv	Mean	1.2
	Contrast	−2.1
	GLDV contrast	2.2
	Entropy	−2.2
L-vv	Mean	−1.2
	Entropy	−2.0
	Homogeneity	1.2
	GLDV contrast	−2.1

The set of selected measures was used as input for the unsupervised classification with hh, hv, vv − L bands and their combinations, hh and hv; hh and vv; hv and vv; hh, hv and vv. The best textural classification for L-band is shown in Figure 5 (hh and vv). The results indicate that not all classes were discriminated on SAR-R99B images when compared with the Surface-Cover Map (see Fig. 2). The latosoil, duricrust (chemical), iron ore duricrust, and lake were not classified. Backscattered L-band responses are no sensitive to these classes. For latosoil the volume scattering effect was predominant, since response was affected by forest canopy over the terrain.

L-band is very sensitive to small-scales variations in surface roughness and the backscatter is affected by the terrain below a vegetation canopy (Tapley, 2002). The dielectric properties of surface materials can also influence on radar return signal. A very
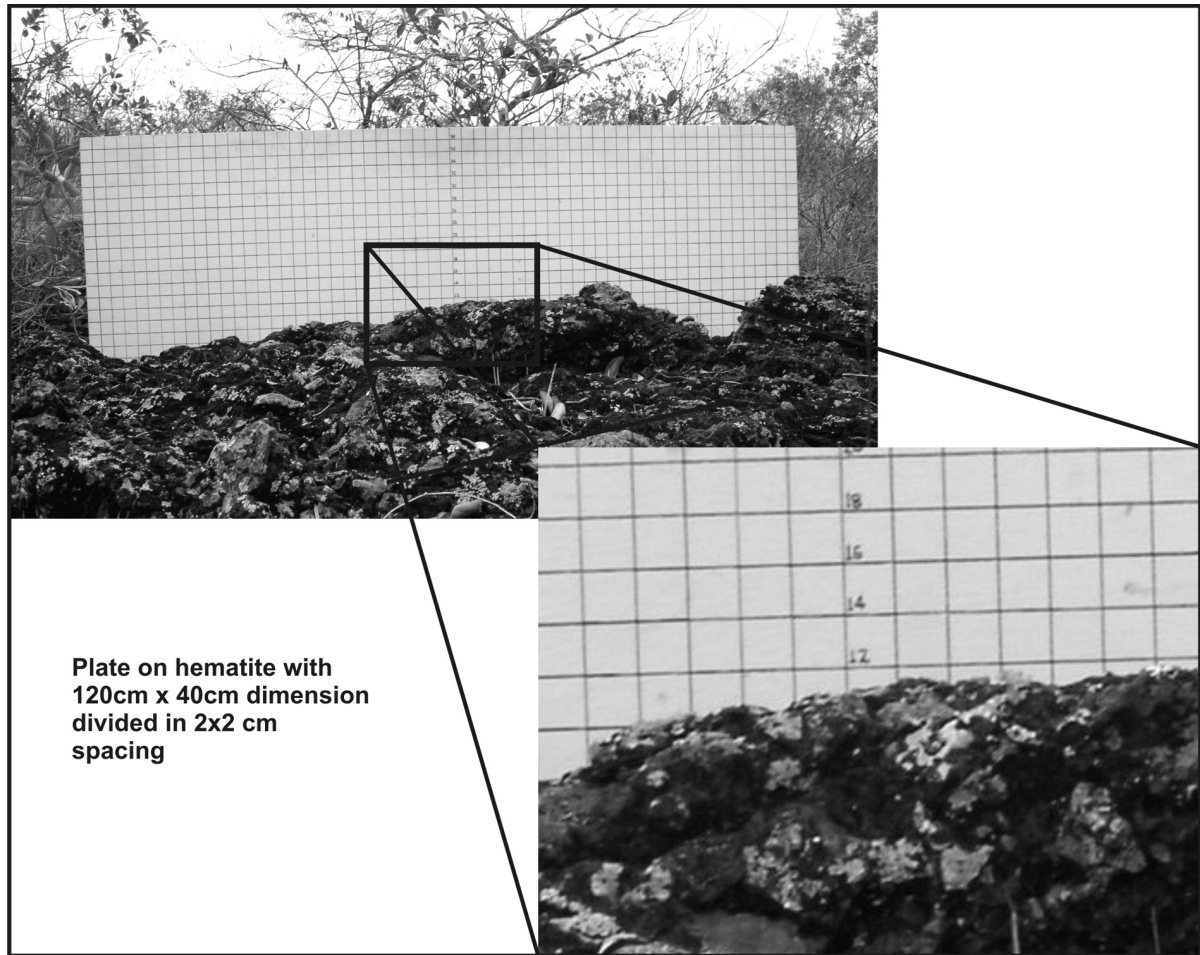
Plate on hematite with 120cm x 40cm dimension divided in 2x2 cm spacing

Figure 4 – Plate on the lateritic cover (120cm length × 40cm height).

low dielectric constant in dry environments allows longer radar wavelengths to penetrate to greater depth (Werle, 1988). Lateritic crusts have capability to retain high water volume on the rainy seasons, but the area was affected by the strong drought, which occurred in the Amazon region, from November 2004 to the end of 2005 (Marengo et al., 2008).

The drought influenced SAR imagery acquisition on June 2005, corresponding to the low rain mean of that year (Fig. 6). At this condition, duricrust (chemical) showed very dry grass vegetation in flat terrains, and the low backscattering can be related to low values of dielectric. This effect was also observed in dry lakes. At normal rain conditions, it was expected the typical aquatic vegetation on lakes, and as a consequence a higher radar responses. Therefore, grasses vegetation appears smooth at L-band, as showed in Figure 7, and it has affected the classification that may results on confusion where dry lakes were incorrectly classified as soil (anthropogenic effects).

Although the soil (anthropogenic effects), duricrust, and hematite were relatively well classified, they presented confusion with other classes. For this reason, the statistical analysis was made between hematite and no hematite classes. Table 3 shows the kappa values for all classifications, where duricrust and soil (anthropogenic effects) were grouped into the "no hematite" class and evaluated with "hematite" class. According to this table, the hh classification was better than vv polarization, while the cross polarization presented the worst result. The best results are for both hh and vv classification, showed by the confusion matrix (Table 4) obtained by test samples based on the field-investigated points, where the rows present the percentage results of the classification and the columns are the truth obtained from random test samples. According these results, hematite showed a god performance on textural classification. The application of the kappa ranking, as proposed by Landis & Koch (1977), supports this results and indicates the following: (1) the best
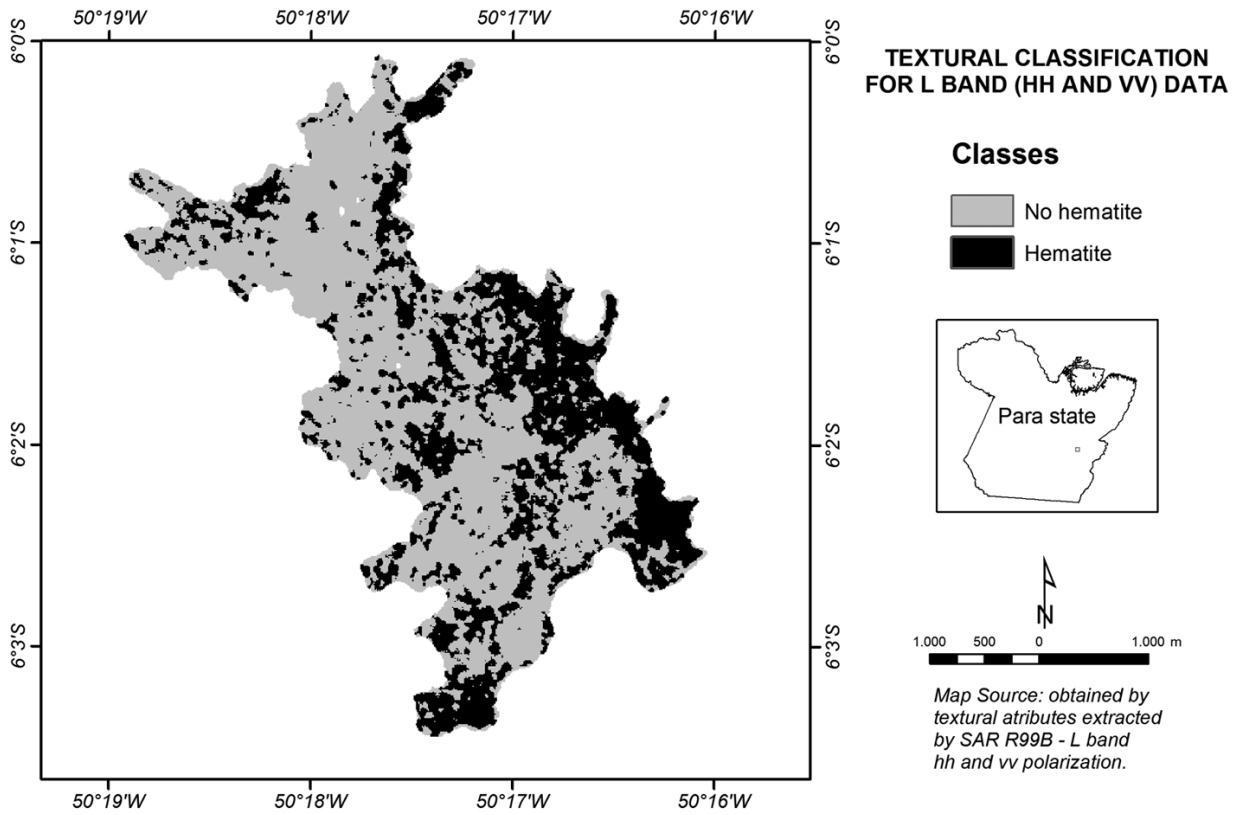
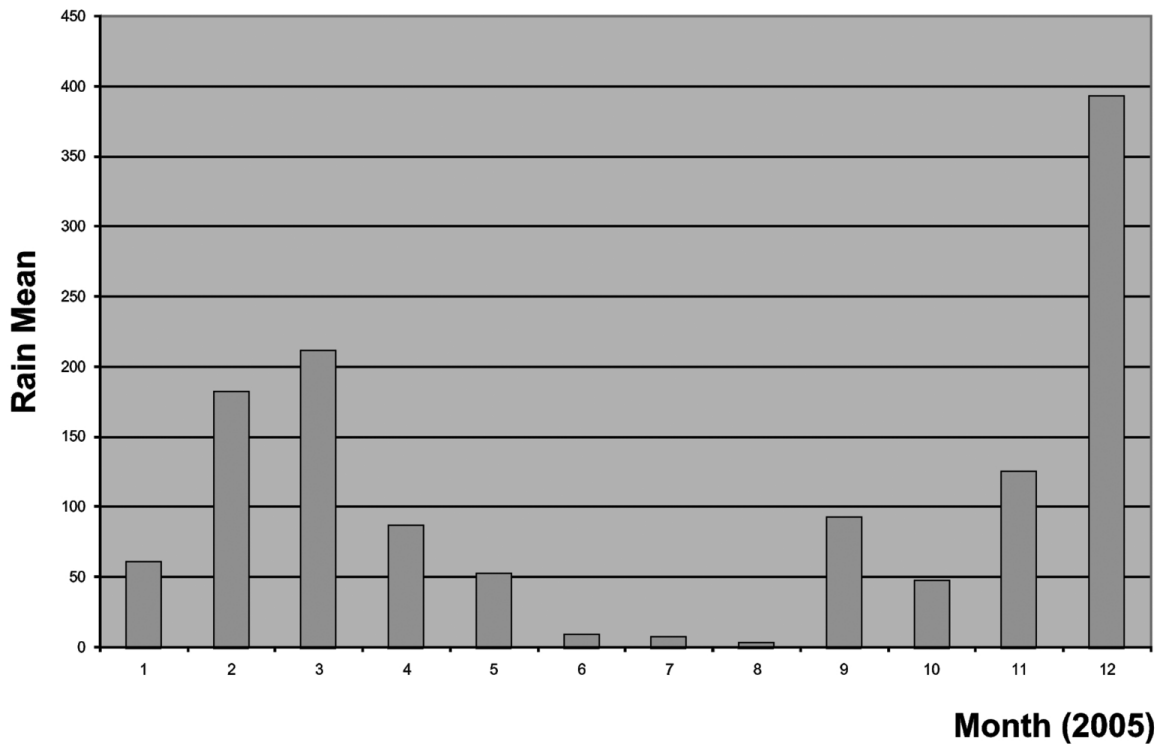**Figure 5** – Textural classification for the L-band (hh and vv) data.

Figure 6 – Rain mean for 2005 year in the area (Source: ANA – National Water Agency).

L - hh

L - vv

L - hv

L - hh-hv-vv (RGB)

Source: SAR R99B
Acquisition: June 2005
Spatial Resolution: 11m
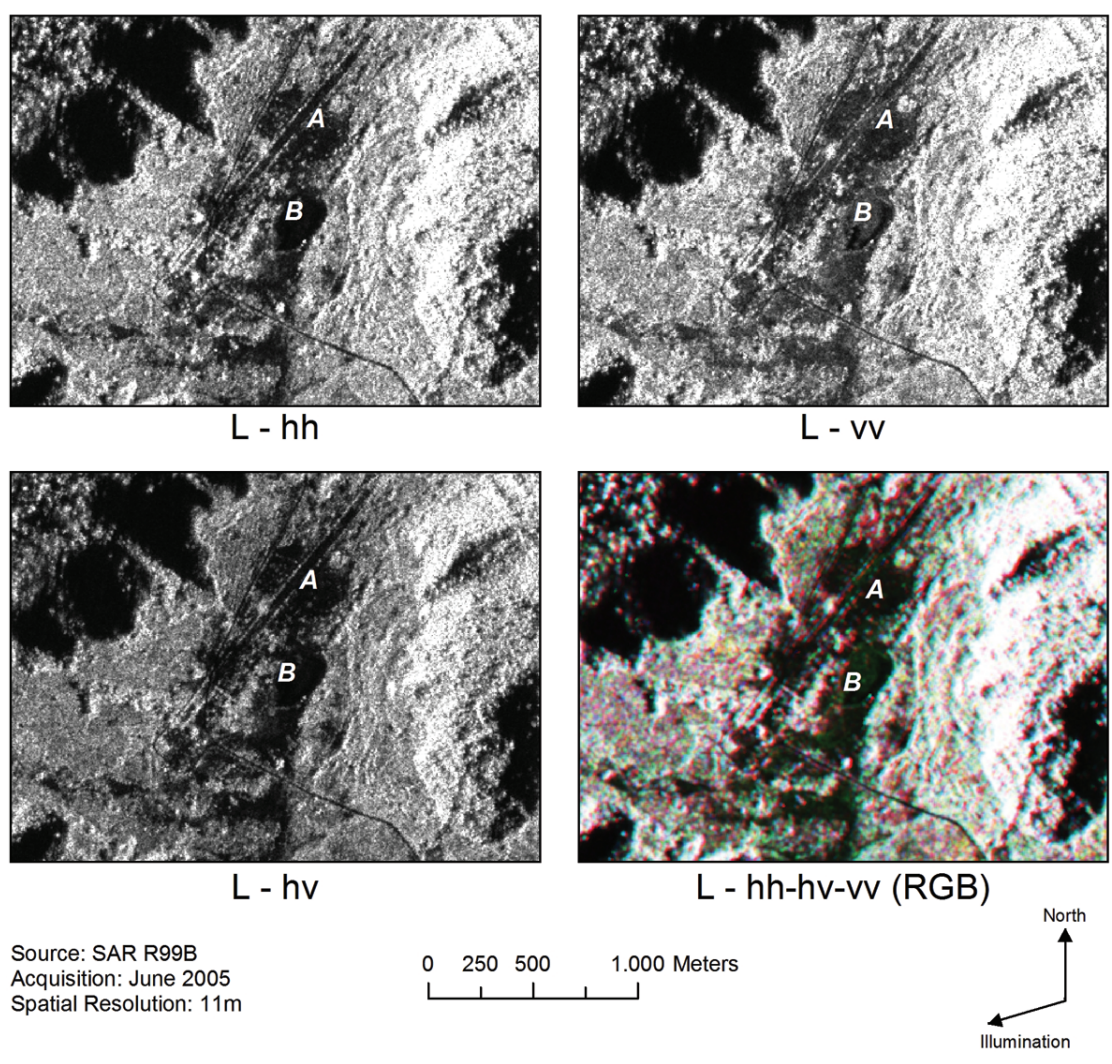
0   250 500   1.000 Meters

North

Illumination

Figure 7 – Responses by polarized L-band radar backscatter for soil (anthropogenic effects) – letter A and dry lake – letter B.

results (very good in the ranking) were obtained when the classifications were based on both polarization under hh and vv, (2) the best classification with only one band occurred when using hh (bad in the ranking), and (3) the cross polarization was considered the worst result for the classifications.

Table 3 – Kappa coefficients for the unsupervised classifications obtained by test samples from field.

SAR data	K (%)	Kappa variance (%)
L-hh-vv	0.720	0.009
L-hv-vv	0.560	0.011
L-hh-hv	0.450	0.013
L-hh-hv-vv	0.400	0.012
L-hh	0.372	0.013
L-vv	0.360	0.013
L-hv	0.320	0.016

Table 4 – Confusion matrix for the classification based on textural attributes extracted from airborne SAR data (hh, hv, and vv).

Classified data	Truth reference data		
	no hematite	hematite	number of pixels
no hematite	80%	20%	30
hematite	24%	76%	20
number of pixels	25	25	50

These results indicate that for N1 deposit hh polarization suffers less attenuation from the vertically arboreal and semi-arboreal vegetation. The hh capacity to penetrate surface materials, which presents a compact horizontal structure, was favored by a large amount of hematite outcrops. Signal polarization has a good performance for vv due the ability to provide better discrimination between targets with similar roughness charac-
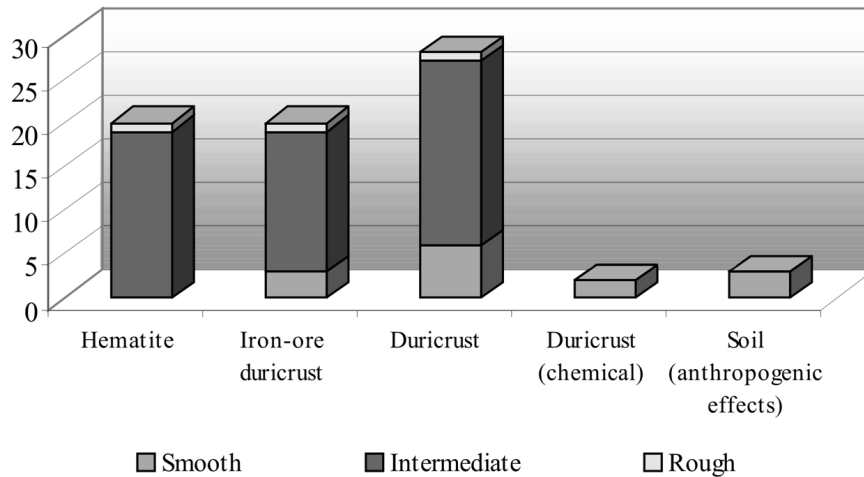
Class and Surface Roughness

**Figure 8** – Roughness classification for all classes.

teristics, like vegetation, soil (anthropogenic effects), duricrust (chemical) and dries lakes. The cross-polarized caused a decreased on kappa values when it added on both hh and vv classifications as it can be derived by a loss of signal radar on cross-polarized response. Also, cross-polarized signal provided a better discrimination between specular and diffuse signal return, like classes covered by dry grasses and arboreal and semi-arboreal vegetation.

In relation to roughness classification, N1 plateau with a relative flat topographic relief and low elevations variation (Fig. 9) is controlled by microrelief. A small range of incident angles occurred since N1 plateau as located in the centre of swath. With regards to L-band, the surface roughness of lateritic crusts derived from 73 *in situ* measurements based on a scheme proposed by Peake & Oliver (1971) were not sensitive to the variations (Fig. 8). According to these results, most classes were classified as intermediate, i.e., the diffuse reflection is observed and this results in medium backscattering SAR. Duricrust (chemical) and soil (anthropogenic effects), presented the best results and were classified as smooth, as expected at L-band. The reduced size particles of these classes, located at flat areas, showed a specular reflection at this wavelength.

The influence of macrotopography was evident on hematite results classification. This class exhibits a stronger influence on relief in eastern segment of the plateaux given by bright returns and shadows (front/back slopes). Further, the 282° look azimuth direction favoured the relief enhancing terrain oriented at NW-SE, with many occurrence of hematite.

CONCLUSIONS

Textures attributes derived from second-order measures (GLCM) from airborne SAR L-band can be used with limitations as a practical tool for a preliminary map. The investigation has shown that textural descriptors were sensitive to the (1) SAR wavelength, (2) SAR polarization, and (3) target parameters (dielectric constant, macro and microtopography). L-band was very sensitive to small-scale areas of vegetation and the surface backscatter was affected by the terrain below this vegetation. For forest canopy on flat terrain, the volume scattering effect was predominant. The hh polarization has better performance than vv to penetrate materials with a compact horizontal structure, like hematite. Already vv polarization presented better performance on discrimination targets with similar roughness characteristics, like vegetation, soil (anthropogenic effects), duricrust (chemical), and dry lakes. The cross-polarized signal caused a decreased on classification results and it can be due to the loss of signal radar on cross-polarized response. The dielectric constant can be affected area submitted targets to drought conditions. The hematite compact structure, on higher areas of the plateau, was sensitive to macrotopography and, and it contributed to discriminate it from others classes. The surface roughness was poorly classified at L-band and most classes were classified as intermediate. Most classes were classified as smooth at specular reflection conditions. From all these factors, it can be observed that the wavelength was the most important factor to discriminate iron-mineralized laterites in N1, as previously observed at C-band in N1. Also, this approach

Figure 9 – DEM generated from topographic curves – N1 plateau.
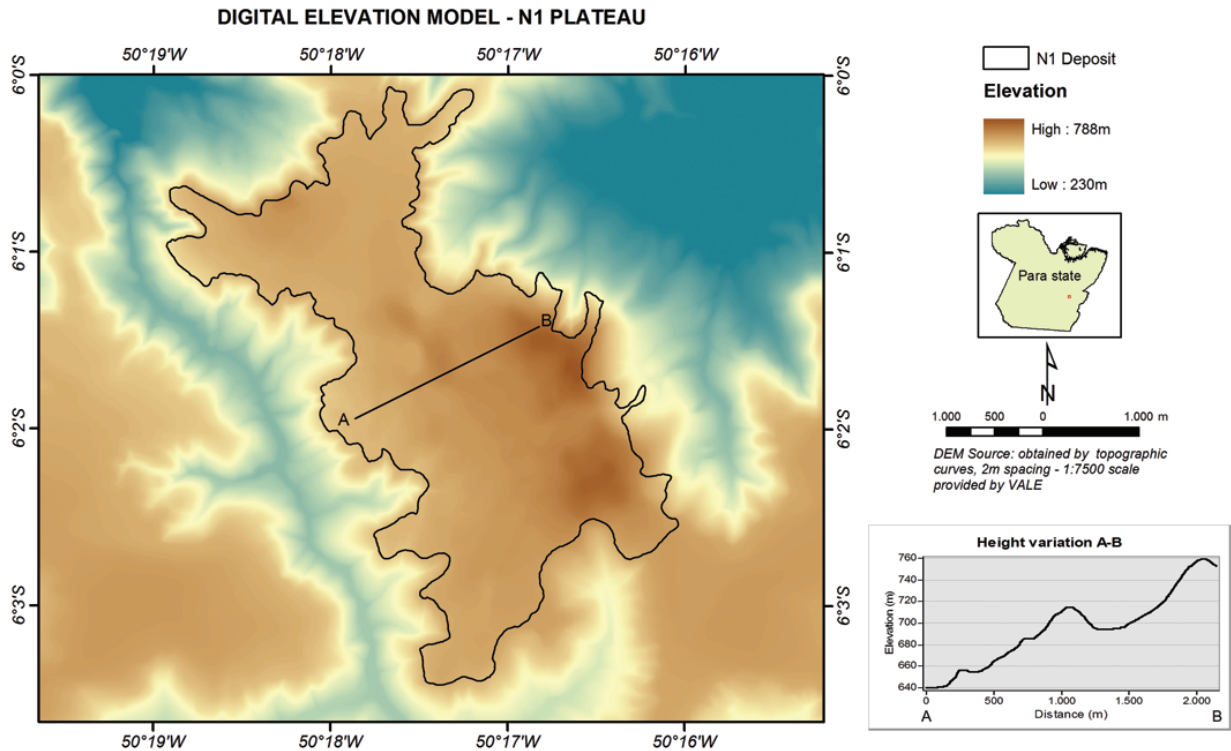
can be used as a practical tool for a preliminary map, which may serve as a guide for detailed iron-mineralized laterites mapping in Carajás, and other minerals, like phosphate-titanium mineralized laterites in Maicuru. Multi-wavelength SAR images is desirable for a better classes discrimination. Finally, an additional approach will deserve attention for future research with use of textural classification derived from polarimetric SAR data.

ACKNOWLEDGEMENTS

REFERENCES

AZZIBROUCK GA, SAINT-JEAN R & PREVOST C. 1997. Analyse de la texture d'une image RADARSAT pour la cartographie géologique dans la Forêt Équatoriale de Ngoutou, est du Gabon. In: Proceedings of Geomatics in the Era of RADARSAT (GER'97), 1997, Ottawa. Proceedings... CD-ROM.

BARALDI A & PARMIGGIANI F. 1995. An investigation of the textural characteristics associated with Gray Level Cooccurrence Matrix statistical parameters. IEEE Trans. Geosc. Remote Sens., 33: 293–304.

BEISIEGEL VR, BERNADELLI AL, DRUMMOND NF, RUFF AW & TREMAINE JW. 1973. Geologia e Recursos Minerais da Serra dos Carajás. Revista Brasileira de Geociências, 3: 215–242.

BENSON AS & DeGLORIA SD. 1985. Interpretation of Landsat-4 Thematic Mapper and Multispectral Scanner data for forest surveys. Photogr. Engineering Remote Sens., 51: 1281–1289.

FOODY GM. 1992. On the compensation for change agreement in image classification accuracy assessment. Photogr. Engineering Remote Sens., 58: 1459–1460.

HARALICK RM. 1979. Statistical and structural approaches to texture. Proceedings of the IEEE, 67: 786–804.

KURVONEN L & HALLIKAINEN MT. 1999. Textural information of multitemporal ERS-1 and JERS-1 SAR images with applications to land and forest type classification in boreal zone. IEEE Trans. Geosc. Remote Sens., 37: 680–689.

LANDIS JR & KOCH GG. 1977. The measures of observer agreement for categorical data. Biometrics, 33: 159–174.

LOBATO LM, ROSIÈRE CA, SILVA RCF, ZUCCHETTI M, BAARS FJ, SEOANE JCS, RIOS FJ, PIMENTEL M, MENDES GE & MONTEIRO

AM. 2005. A mineralização hidrotermal de ferro da Província Mineral de Carajás – Controle estrutural e contexto na evolução metalogenética da província. In: Caracterização de depósitos minerais em distritos mineiros da Amazônia. ADIMB/DNPM, Ed., DNPM-CT/MINERAL-ADIMB: Brasília, 2: p. 20–92.

MARENGO JA, NOBRE CA, TOMASELLA J, CARDOSO MF & OYAMA MD. 2008. Hydro-climatic and ecological behaviour of the drought of Amazonia in 2005. Philosophical Transactions of the Royal Society of London, 363(1498): 1773–1778.

MATHER PM. 1987. Computer processing of remotely-sensed images: an introduction. John Wiley, Chichester, U.K., 325 p.

MEIRELLES EM, HIRATA WK, AMARAL AF, MEDEIROS FILHO CA & GATO WC. 1984. Geologia das folhas Carajás e Rio Verde, Província Mineral dos Carajás, Estado do Pará. In: Brazilian Congress of Geology, 33., 1984, Rio de Janeiro. Annals... Rio de Janeiro: SBG, 1984, p. 2164–2174.

MORAIS MC, PARADELLA WR & FREITAS CC. 2002. An assessment of the discrimination of iron-mineralized laterites in the Amazon region (Carajás Province) based on textural attributes from C-band airborne SAR data. Asian J. Geoinfo., 3: 11–20.

PARADELLA WR, SILVA MFF, ROSA NA & KUSHIGBOR CA. 1994. A geobotanical approach to the tropical rain forest environment of the Carajás Mineral Province (Amazon Region, Brazil), based on digital TM-Landsat and DEM data. Int. J. Remote Sens., 15: 1633–1648.

PARADELLA WR, BIGNELLI PA, VENEZIANI P, PIETSCH RW & TOUTIN T. 1997. Airborne and spaceborne Synthetic Aperture Radar (SAR) integration with Landsat TM and gamma ray spectrometry for geological mapping in a tropical rainforest environment, the Carajás Mineral Province, Brazil. Int. J. Remote Sens., 18: 1483–1501.

PARADELLA WR, SANTOS AR, VENEZIANI P, SANT'ANNA MV & MORAIS MC. 2000. Geological investigation using RADARSAT-1 images in the tropical rainforest environment of Brazil. Canadian Journal of Remote Sensing, 26: 82–90.

PEAKE WM & OLIVER TL. 1971. The response of terrestrial surfaces at microwave frequencies. Technical Report. Columbus, Ohio, p. 2440–2447.

RENNÓ CD, FREITAS CC & SANT'ANNA SJS. 1998. A system for region classification based on textural measures. In: Brazilian Remote Sensing Symposium, 9., 1998, Santos. Annals... Santos: INPE, 1998, on-line.

RESENDE NP & BARBOSA ALM. 1972. Relatório de Pesquisa de Minério de Ferro, Distrito Ferrífero da Serra dos Carajás, Estado do Pará. AMZA. Final Report, v. 1, 248 p.

SCHRÖDER R, PULS J, HAJNSEK I, JOCHIM F, NEFF T, KONO J, PARADELLA WR, SILVA MM, VALERIANO DM & COSTA MPF. 2005. MAPSAR: a small L-band SAR mission for land observation. Acta Astronautica, 56: 35–45.

SHANMUGAN KS, NARAYANAN V, FROST VS, STILES JA & HOLTZMAN JC. 1981. Textural Features for Radar Images. IEEE Trans. Geosc. Remote Sens., 19: 153–156.

SILVA MFF, MENEZES NL, CAVALCANTE PB & JOLY CA. 1986. Estudos Botânicos: histórico, atualidade e perspectivas. In: Carajás: desafio político, ecologia e desenvolvimento. CNPq/Brasiliense. Cap. 8, p. 185–206.

TAPLEY IJ. 2002. Radar Imaging. In: PAPP E (Ed.). Geophysical and remote sensing methods for regolith exploration. CRC LEME. Open File Report 144, p. 22–32.

TOLBERT GE, TREMAINE JW, MELCHER GC & GOMES CB. 1971. The recently discovered Serra dos Carajás iron deposits, Northern Brazil. Economic Geology, 66: 985–994.

ULABY FT, KOUYATE F, BRISCO B & WILLIAMS THL. 1986. Textural information in SAR images. IEEE Trans. Geosc. Remote Sens., 24: 235–245.

WELCH RM, KUO SS & SENGUPTA SK. 1990. Cloud and surface textural features in polar region. IEEE Trans. Geosc. Remote Sens., 28: 520–528.

WERLE D. 1988. Radar remote sensing: a training manual. Ottawa: Dendron Resource Surveys, 300 p.

WESKA JS, DYER CR & ROSENFELD A. 1976. A comparative study of texture measures for terrain classification. IEEE Trans. Syst. Man Cybern., 4: 269–285.

WOODING MG, ZMUDA AD & ATTEMA E. 1993. An overview of SAREX'92 data acquisition and analysis of the tropical forest environment. In: Workshop of SAREX-92 (South American Radar Experiment), 6-8., 1993, Paris. Proceedings... Paris: ESA, 1993, p. 3–14.

YANASSE CCF, FRERY AC, SANT'ANNA SJS, HERNANDES FILHO P & DUTRA LV. 1993. Statistical analysis of SAREX data over Tapajós – Brazil. In: Workshop of SAREX-92 (South American Radar Experiment), 6-8., 1993, Paris. Proceedings... Paris: ESA, 1993, p. 25–40.

NOTES ABOUT THE AUTHORS

Maria Carolina de Morais. Geological Engineer (School of Mines, Federal University of Ouro Preto, 1995), Master's Degree in Remote Sensing at the National Institute for Space Research (INPE, 1998), doctoral student at the Federal University of Ouro Preto in Crustal Evolution and Natural Resources, concentration area Environmental Geology and Conservation of Natural Resources. Experience in Geosciences, with emphasis on Remote Sensing, GIS, acting on the following topics: Digital mapping through satellite imagery, multispectral and radar, Geophysical data in order to mineral exploration and Natural resource management.

Paulo Pereira Martins Junior. Geologist (Geosciences Institute – Federal University of Rio de Janeiro, 1970), holds a Doctorate, Dr.Sc.T., in Géologie Dynamique – Université Pierre et Marie Curie – Paris VI, Laboratoire de Géologie Dynamique in 1977. Professor-Researcher at the Federal University of Ouro Preto and Science and Technology Researcher at Minas Gerais Tecnological Center Foundation – CETEC. Experience on the following topics: Epistemology, Agrarian and Environmental Geosciences, Modeling watersheds environmental management, Ecology-Economy, System development for Architecture of Knowledge, Cartographic developments in ecology, energy and economy and Certification Methods Geo-environmental and economic.

Waldir Renato Paradella. Geologist (University of São Paulo – IGUSP, 1973), Master's Degree in Remote Sensing (National Institute for Space Research – INPE, 1976), Ph.D. in General Geology (University of São Paulo – IGUSP, 1983) and post-doctoral at CNPq (1988-1989) and CIDA – Canadian International Development Agency (1995-1996) in Canada. III Researcher holder of the Remote Sensing Division (RSD) of INPE. Experience in the Geosciences, Applications of radar images in Geology and Cartography, with emphasis in Radargrammetry, Polarimetry, and Interferometry. Coordinator of radar symposia in 2000 (Rio de Janeiro) and 2008 (Oslo, Norway) of the International Geological Congress.